

Molecular Proximity of Cystic Fibrosis Transmembrane Conductance Regulator and Epithelial Sodium Channel Assessed by Fluorescence Resonance Energy Transfer^{*[5]}

Received for publication, September 28, 2007 Published, JBC Papers in Press, October 3, 2007, DOI 10.1074/jbc.M708089200

Bakhrom K. Berdiev^{†S1}, Estelle Cormet-Boyaka[¶], Albert Tousson^{S||}, Yawar J. Qadri[‡], Henderika M. J. Oosterveld-Hut^{**}, Jeong S. Hong^S, Patricia A. Gonzales^{‡‡}, Cathy M. Fuller[‡], Eric J. Sorscher^{SS}, Gergely L. Lukacs^{¶¶}, and Dale J. Benos[‡]

From the Departments of [†]Physiology & Biophysics, ^SCell Biology, ^{||}High Resolution Imaging Facility, and ^{SS}Gregory Fleming James Cystic Fibrosis Research Center, The University of Alabama at Birmingham, Birmingham, Alabama 35294-0005, the [¶]Division of Pulmonary, Critical Care, and Sleep Medicine, Davis Heart and Lung Research Institute, The Ohio State University, Columbus, Ohio 43210-1252, ^{**}Lambert Instruments, Turfweg 4, Leutingewolde 9313 TH, The Netherlands, the ^{‡‡}Laboratory of Kidney & Electrolyte Metabolism, NHLBI, National Institutes of Health, Bethesda, Maryland 20892-1603, and the ^{¶¶}Laboratory of Laboratory Medicine and Pathobiology, Program in Cell and Lung Biology, The Hospital for Sick Children Research Institute, University of Toronto, Ontario M5G 1X8, Canada

We present the evidence for a direct physical association of cystic fibrosis transmembrane conductance regulator (CFTR) and epithelial sodium channel (ENaC), two major ion channels implicated in the pathophysiology of cystic fibrosis, a devastating inherited disease. We employed fluorescence resonance energy transfer, a distance-dependent imaging technique with capability to detect molecular complexes with near angstrom resolution, to estimate the proximity of CFTR and ENaC, an essential variable for possible physical interaction to occur. Fluorescence resonance energy transfer studies were complemented with a classic biochemical approach: coimmunoprecipitation. Our results place CFTR and ENaC within reach of each other, suggestive of a direct interaction between these two proteins.

CF² is the most common lethal autosomal recessive disorder in Caucasians. It is caused by mutations in the CFTR protein (1–3), a Cl⁻ channel that is widely expressed in epithelia (4). In the airways of patients with CF, mutations in the *cftr* gene lead to the production of poorly hydrated airway surface liquid interface, thick and sticky mucus, which in turn reduces mucociliary clearance and promotes bacterial colonization and sec-

ondary infections (5). The gastrointestinal abnormalities present earlier with failure to thrive; reduced fluid secretion in the pancreatic ducts compromises digestive enzyme release into the duodenum, resulting in poor nutrition (5, 6). However, the airway pathology is the major cause of CF mortality (5–7).

Although CFTR is primarily an anion channel (4, 8–10), these major symptoms are not solely due to deficiencies in anion secretion. Absorption of the obligate cation Na⁺ across the apical membrane of the respective epithelium also contributes to the pathology (5, 7, 11). Some of the earliest electrophysiological studies of CF patient airways demonstrated that an amiloride-sensitive Na⁺ transport pathway contributed to the raised transepithelial potential difference across CF nasal epithelia (12). This sensitivity to the diuretic amiloride suggested an involvement of the ENaC family of proteins. Recently, further experimental evidence supporting a role for ENaC in airway hydration has been obtained in mice overexpressing β -ENaC (13). These animals develop a “CF-like” airway disease, which was attributed to over-absorption of Na⁺. CFTR knock-out mice recapitulated the gastrointestinal abnormalities but did not show this airway pathology (13). Thus, CFTR and ENaC both contribute to the pathology of CF, although only CFTR is affected by the genetic mutations.

These facts suggest that these two proteins are functionally interrelated. Previous studies have suggested that CFTR down-regulates ENaC function (14–18), thus restricting absorption and shifting fluid balance across the epithelium in favor of net secretion (7). In CF, however, the reverse process happens: ENaC is freed from the constraint exerted by CFTR, which is either non-functional or absent in CF, and now causes increased absorption of Na⁺ across the epithelium, with Cl⁻ following via paracellular pathways. The result is dehydration of the airway surface fluid seen in CF patients (5).

The presence of a functional link between CFTR and ENaC has been reported by many laboratories in a number of experimental situations (14–16, 19–23) and is seen clinically with the nasal potential difference used to diagnose CF (12). However, the existence of this interaction *in vitro* has been questioned

* This work was supported by National Institutes of Health Grants 2R01-DK37206-15, P50 DK53090-05, and R01-DK075302 CFF/CFPT. The costs of publication of this article were defrayed in part by the payment of page charges. This article must therefore be hereby marked “advertisement” in accordance with 18 U.S.C. Section 1734 solely to indicate this fact.

[5] The on-line version of this article (available at <http://www.jbc.org>) contains supplemental Figs. S1–S4.

¹ To whom correspondence should be addressed: Dept. of Cell Biology, The University of Alabama at Birmingham, 1918 University Blvd., MCLM 725, Birmingham, AL 35294-0005. Tel.: 205-934-6186; Fax: 205-934-2377; E-mail: berdiev@uab.edu.

² The abbreviations used are: CF, cystic fibrosis; CFTR, cystic fibrosis transmembrane conductance regulator; ENaC, epithelial sodium channel; FRET, fluorescence resonance energy transfer; E, FRET efficiency; ECFP, enhanced cyan fluorescent protein; EYFP, enhanced yellow fluorescent protein; EGFP, enhanced green fluorescent protein; co-IP, co-immunoprecipitation; FLIM, fluorescence lifetime imaging microscopy; PBS, phosphate-buffered saline; Ab, antibody.

(24–26), and the mechanism underlying this interaction is poorly defined.

In the present study, we have addressed the issue of whether or not there is direct interaction between ENaC and CFTR using an independent biophysical approach; *i.e.* FRET imaging. FRET exploits the exquisite sensitivity of fluorescence measurements to detect the presence of molecular complexes with near angstrom resolution. Using a standard FRET pair, with enhanced cyan fluorescent protein (ECFP) as a donor and enhanced yellow fluorescent protein (EYFP) as an acceptor, we have found that co-transfection of ECFP-CFTR with EYFP-tagged ENaC subunits resulted in significant FRET efficiencies (*E*). In contrast, co-transfection of ENaC subunits with ECFP-CLCN1, an ion channel not found to functionally couple with ENaC, resulted in little to no FRET (*E* < 0.5%), an outcome comparable to negative controls (ECFP and EYFP co-transfected cells). Co-immunoprecipitation (Co-IP) experiments showed that $\alpha\beta\gamma$ -ENaC consistently co-immunoprecipitated with CFTR. These results place CFTR and ENaC proteins in very close proximity to each other, consistent with a direct interaction of these two proteins. This renders plausible a possibility that these two proteins interact directly *in vivo* to contribute to CF airway pathology.

MATERIALS AND METHODS

Cell Culture—Human embryonic kidney 293T (HEK293T) cells (kind gift of Dr. K. Kirk, University of Alabama at Birmingham) were maintained in Dulbecco's modified Eagle's medium (Invitrogen) supplemented with 10% fetal bovine serum (HyClone, Logan, UT) and penicillin/streptomycin (Invitrogen) in polystyrene flasks at 37 °C with 5% CO₂. One day before transfection, the cells were subcultured using trypsin (Mediatech, Herndon, VA) and ~50,000 cells were seeded on 1:10 diluted poly-L-lysine (Sigma)-coated coverslips (Fisher Scientific, Pittsburgh, PA).

Transient Transfection—Transient transfections of the cells with construct(s) of interest were performed using Lipofectamine 2000 reagent (Invitrogen) following the manufacturer's recommended protocol (27). Briefly, 1 μ l/200 ng of DNA of Lipofectamine 2000 reagent was diluted with 100 μ l of Opti-MEM® I (Invitrogen) and incubated at room temperature for 5 min. Separately, 200 ng of each DNA construct was diluted with 100 μ l of Opti-MEM® I (Invitrogen). After 5-min incubation, the diluted DNA constructs were combined with Lipofectamine 2000 and allowed to complex for 20 min. After incubation the transfection solution was added to the cells in Opti-MEM® I. The cells were incubated for 5 h at 37 °C in a CO₂ incubator followed by a change of the transfection solution to regular growth medium without antibiotics. Forty-eight hours after transfection, the cells were gently rinsed with 1 \times phosphate-buffered saline (PBS, Invitrogen) and fixed for 15 min at room temperature with 4% paraformaldehyde (prepared from 20% EM Grade solution, Electron Microscopy Services, Hatfield, PA). Cells then were rinsed three times with 1 \times PBS and mounted on glass microscope slides (Fisher Scientific) using 0.2% *n*-propyl gallate (Sigma) in 9:1 glycerol/PBS (v/v). The same protocol was used to transfect the cells for co-immuno-

precipitation experiments; the DNA/Lipofectamine 2000 ratio was 1 μ g/2.5 μ l.

Generation of the Fluorophore-tagged CFTR and ENaC cDNAs—We have restricted our study to the N-terminal tail of CFTR and C termini of $\alpha\beta\gamma$ -ENaC. Previous studies have shown that an interference with the C-terminal tail of CFTR might lead to its improper localization due to disruption of a PDZ binding motif (28). Similarly, manipulation of N termini of $\alpha\beta\gamma$ -ENaC affects its gating properties (18, 29). The CFTR N-terminally tagged with enhanced green fluorescent protein (EGFP-CFTR) was a kind gift of Dr. B. Stanton, Dartmouth Medical School (30). The EGFP was exchanged with enhanced cyan fluorescent protein CFTR (ECFP-CFTR) following *NheI*/*XhoI* (New England Biolabs, Ipswich, MA or Promega, Madison, WI) digestion (see Fig. 1C). Human Chloride Channel 1 (CLCN1) tagged N-terminally with ECFP (ECFP-CLCN1) was a kind gift of Dr. Christoph Fahlke (Dept. of Neurophysiology, Medizinische Hochschule Hannover, Hannover, Germany) (31). cDNA constructs of human α -ENaC, β -ENaC, and γ -ENaC subunits with C-terminal EYFP were generated by PCR amplification of the genes of interest and cloning into the vector pEYFP-N1 (BD Biosciences Clontech, Palo Alto, CA) using *XhoI* and *BamHI* restriction sites (27). Positive control (ECFP-EYFP) was generated by fusion of ECFP to EYFP-N1 vector using *XhoI* and *BamHI* restriction sites through a 7-amino acid linker (SGLRSRA). All constructs were verified by direct sequencing prior to use.

ENaC Antibodies—Rabbit polyclonal antibodies (Abs) were generated against synthetic peptides in collaboration with Dr. Mark Knepper (National Institutes of Health). Antigenic peptides with the sequences, α -hENaC, LMKGNKREEQGLGPEP-AAPQQPTC; β -hENaC, CNYDSLRLQPLDVIESDSEGDAL; and γ -hENaC, CNTLRLDSAFSSQLTDTQLTNEF, were synthesized by Lofstrand Laboratories (Gaithersburg, MD). The peptides correspond to human sequences, chosen to maximize immunogenicity, to minimize likely cross reactions with other eukaryotic proteins, and to avoid common post-translational modifications as described (32). All peptides were high-performance liquid chromatography-purified. The peptides were conjugated to a carrier protein keyhole limpet hemocyanin and injected into rabbits using a standard protocol (Antibodies Inc., Davis, CA). Antisera from test bleeds, production bleeds, and final exsanguination were affinity-purified and tested on immunoblots from human kidney cortex and medulla (not shown). These immunoblots showed single bands in the range of 80–90 kDa consistent with previous anti-ENaC Abs directed to rodent proteins (33).

Western Blot Analysis of CFTR and ENaC (34, 35). CFTR—HEK293T cells were transfected with 2 μ g of ECFP-CFTR construct. 48 h post-transfection, cells were lysed with radioimmune precipitation assay buffer (Pierce) complemented with Complete® protease inhibitor mixture (Roche Biochemical, Mannheim, Germany) at 4 °C. After centrifugation (15,800 \times *g* for 10 min at 4 °C) non-soluble material was discarded. 100 μ g of total cell lysate was analyzed on a 6% protein gel (Invitrogen). The protein gel was blotted onto a polyvinylidene difluoride membrane (Bio-Rad) and probed with 1:10,000 diluted polyclonal Ab against the second nucleotide binding domain of

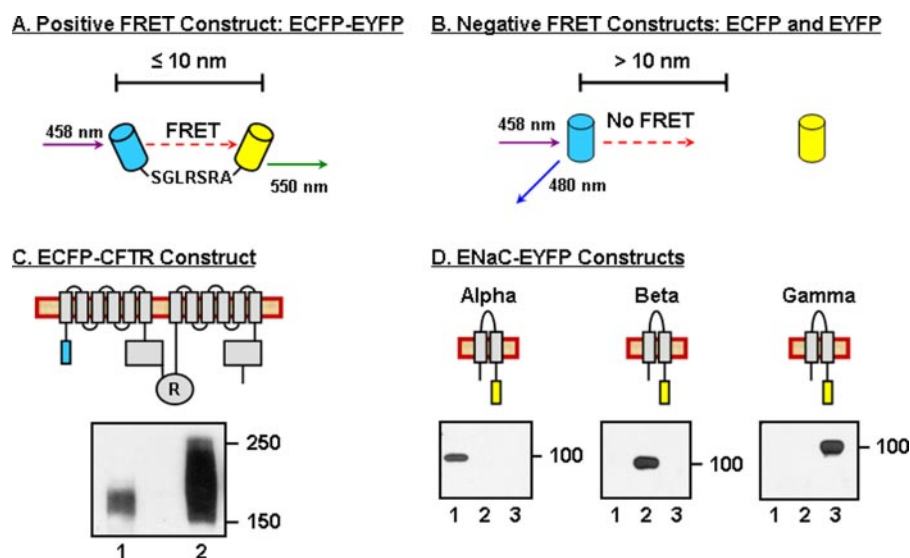


FIGURE 1. Schematic representations of control, tagged CFTR, and tagged ENaC constructs. A, positive FRET construct refers to a construct in which ECFP was fused to EYFP through a linker consisting of seven amino acids, SGLRSRA. The FRET principle is based on the following concept: if two fluorescent proteins, a donor and acceptor, are sufficiently close (≤ 10 nm), radiation-less (*i.e.* not mediated by photons) transfer of energy from donor to acceptor can be observed after excitation of the donor. The efficiency of energy transfer is directly related to the distance between the donor and acceptor. If the fluorophores are more than 10 nm apart, no FRET will be detected (B). The negative control depicts the constructs encoding separately ECFP and EYFP. C, ECFP-CFTR construct with corresponding Western blot analysis. Western blot was performed using polyclonal Ab against NBD2 domain of CFTR and probed with anti-rabbit horseradish peroxidase using chemiluminescence. D, ENaC fusion constructs and corresponding Western blot analysis. Each blot contained 10 μ l of lysate of α (lane 1), β (lane 2), and γ -ENaC (lane 3).

CFTR (University of Alabama at Birmingham Cystic Fibrosis Research Center) and probed with anti-rabbit horseradish peroxidase (Dako, Denmark A/S) using chemiluminescence.

ENaC—HEK293T cells were transfected with 1 μ g of ENaC construct. Forty-eight hours post-transfection, cells were lysed with radioimmune precipitation assay buffer with Complete[®] protease inhibitor mixture (Roche Applied Science) at 4 °C. After centrifugation (15,800 \times g for 10 min at 4 °C) non-soluble material was discarded. 2 μ g of total cell lysate was analyzed on 4–20% gradient NuPage gel (Invitrogen); a Bio-Rad Broad range prestained marker was used as the molecular weight standard. The protein gel was blotted onto polyvinylidene difluoride membrane and probed with 1:10,000 dilution of α -ENaC-specific Ab (lot #7038-4, 0.9 μ g/ml stock solution), 1:10,000 dilution of β -ENaC-specific Ab (lot #7040-4, 0.84 μ g/ml stock solution), and 1:10,000 dilution of γ -ENaC-specific Ab (lot #7042-4, 2.37 μ g/ml stock solution). These polyclonal anti-ENaC-specific Abs were applied in 5% dry milk in PBS/Tween (0.1%), overnight. After incubating the blot with ENaC Abs, it was incubated with 1:10,000 diluted anti-rabbit horseradish peroxidase (Dako) and developed using West Pico (Pierce).

CFTR and ENaC Co-immunoprecipitation—CFTR and ENaC co-immunoprecipitation were performed as described previously (35). Briefly, HEK293T cells were transfected with CFTR and appropriate combinations of ENaC subunits. Forty-eight hours post-transfection, cells were lysed with 0.2% Triton X-100 in PBS complemented with Complete[®] protease inhibitor mixture (Roche Applied Science) at 4 °C. After centrifugation (15,800 \times g for 10 min at 4 °C) non-soluble material was discarded, and the supernatant was incubated with 1 μ g of C-terminal CFTR monoclonal Ab clone 24-1 (R&D Systems,

Minneapolis, MN) cross-linked to A/G-agarose beads (Santa Cruz Biotechnology, Santa Cruz, CA) for 2 h. After incubating the lysates with cross-linked Ab, the beads were pelleted and washed three to five times in PBS containing 1% Triton X-100. Precipitated CFTR and bound proteins were analyzed on SDS-PAGE, transferred to a polyvinylidene difluoride membrane and the samples were processed for Western blotting using Abs raised against ENaC and CFTR.

FRET Imaging—The acceptor photobleaching approach was performed as previously described (27, 36). Briefly, images were acquired using the Leica Confocal Scanning System (Exton, PA) TCS SP2 outfitted with a Leica DMRXE upright microscope, an argon laser, and 100 \times 1.4 numerical aperture Plan Apochromatic oil immersion objective. ECFP and EYFP fluorescence were excited with 458 and 514 nm laser light, respectively. Dual excita-

tion was achieved by a dual dichroic (DD458/514) mirror in the excitation path. The emissions for ECFP and EYFP were collected using 465–505 and 525–600 nm bandpass windows, respectively. Fixed samples were imaged within 3 days. We noticed an increase in background fluorescence if fixed samples were processed after a long period (>7–10 days) of storage. The regions of interest in cells expressing both fluorophores were photobleached using 514 nm laser light to 30% of original intensity. ECFP and EYFP images were taken both before and after acceptor photobleaching. FRET efficiency (E) was calculated using Leica software: $E = D_{\text{post}} - D_{\text{pre}}/D_{\text{post}}$, where D_{pre} and D_{post} are ECFP emission before and after regional photobleaching.

FLIM—The images were taken with the LIFA system (Lambert Instruments, The Netherlands), a frequency domain FLIM system, attached to a Nikon TE2000 wide field fluorescence microscope with 100 \times 1.49 numerical aperture objective. A 443 nm modulated LED was used as a light source, and 12 phase-step images were taken at the frequency of 40 MHz with the modulated ICCD (intensified charge-coupled device) camera. By using the filter cyan GFP only the donor emission was measured. In the resulting images, the intensity is shown in grayscale analog-to-digital units, and the lifetime from phase is in pseudocolors (nanoseconds).

RESULTS

Expression, Fluorescence Imaging, and Functional Analysis of the Fluorophore-tagged Constructs—Western blot detection of tagged CFTR and ENaC constructs was performed to test whether the fusion of the 27-kDa ECFP or EYFP tags affected protein expression. The blot in Fig. 1C demonstrates the bands

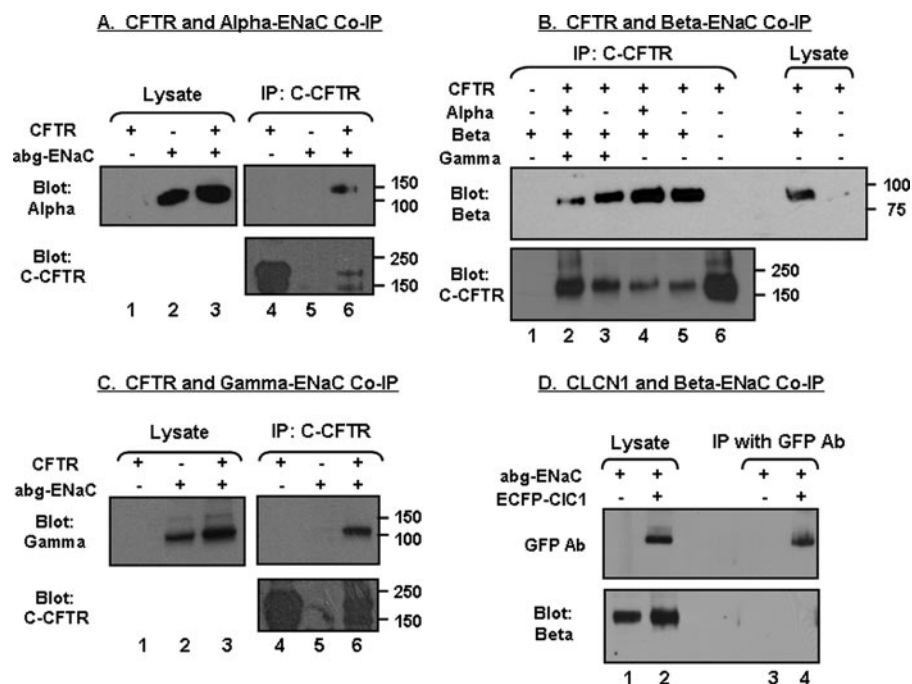


FIGURE 2. ENaC subunits interact with CFTR. A, α -ENaC could be co-immunoprecipitated using a CFTR Ab when co-expressed with CFTR (lane 6). No α -ENaC signal was detected when α -ENaC and CFTR were expressed alone (lanes 4 and 5). The left portion of the panel (lanes 1–3) shows that α -ENaC can only be detected when expressed in cells. Therefore, α -ENaC is not endogenously expressed in those cells (see lanes 2 and 3). B, β -ENaC could be co-immunoprecipitated with CFTR when co-expressed in cells. Only simultaneous presence of both CFTR and β -ENaC, with the combinations of α/β -ENaC, β/γ -ENaC, or β -ENaC with CFTR (lanes 2–5), resulted in Co-IP signal. The absence of either CFTR (lane 1) or β -ENaC (lane 6) eliminated the Co-IP signal. The presence (lane 7) or the absence (lane 8) of β -ENaC signal was confirmed in lysates. C, γ -ENaC could be Co-IP using a CFTR Ab when co-expressed with CFTR (lane 6). No γ -ENaC signal was detected when ENaC subunits and CFTR were expressed alone (lanes 4 and 5) indicating that γ -ENaC does not bind nonspecifically to the beads. The left portion of the panel (lanes 1–3) shows that γ -ENaC is detected only in cells transfected with γ -ENaC construct. D, β -ENaC does not Co-IP with the Cl^- channel ECFP-CLCN1 when co-expressed in cells. Anti-GFP monoclonal Ab JL-8 (BD Living Colors) was used to IP CLCN1, and the blot was probed with the β -ENaC Ab. The expression of CLCN1 in the cells was confirmed using GFP Ab (lanes 2 and 4). An Ab against β -ENaC failed to detect a co-IP signal in IP of cells co-expressing β -ENaC and CLCN1 (lane 4, bottom panel). The expression of β -ENaC in the lysates was confirmed (lanes 1 and 2). These experiments were repeated at least three times, and similar results were obtained.

corresponding to the expected molecular mass of untagged CFTR (lane 1) and the N-terminally tagged construct with a 27-kDa fluorescence tag, ECFP (lane 2, ECFP-CFTR). Similarly, the bands corresponding to the molecular mass of ENaCs with 27-kDa fluorescence tags were observed in cells expressing tagged ENaC subunits (Fig. 1D). We next tested whether fusion of the ECFP or EYFP tags altered the proper plasma membrane targeting of CFTR and ENaC constructs. We found that the expression of CFTR construct predominantly delineated the plasma membrane. This staining suggests that the addition of fluorescence tags does not interfere with the trafficking of CFTR (data not shown). The functional expression of fluorophore-tagged CFTR constructs revealed no alteration in its function as a Cl^- channel (data not shown) in agreement with previously published findings (28). A predominant endoplasmic reticulum staining was observed for ENaC by immunofluorescence (data not shown) and is characteristic of the poor trafficking of these proteins. However, amiloride-sensitive currents characteristic of functional ENaC channels were recorded from cells transiently transfected with tagged ENaC subunits (data not shown and Refs. 27, 37, 38). These data suggest that a population of ENaC proteins reaches the plasma membrane of transfected cells. Cotransfection of CFTR and ENaC constructs

showed colocalization of the two proteins suggesting that they can traffic to the plasma membrane (supplemental Fig. S1).

showed colocalization of the two proteins suggesting that they can traffic to the plasma membrane (supplemental Fig. S1).

showed colocalization of the two proteins suggesting that they can traffic to the plasma membrane (supplemental Fig. S1).

showed colocalization of the two proteins suggesting that they can traffic to the plasma membrane (supplemental Fig. S1).

showed colocalization of the two proteins suggesting that they can traffic to the plasma membrane (supplemental Fig. S1).

showed colocalization of the two proteins suggesting that they can traffic to the plasma membrane (supplemental Fig. S1).

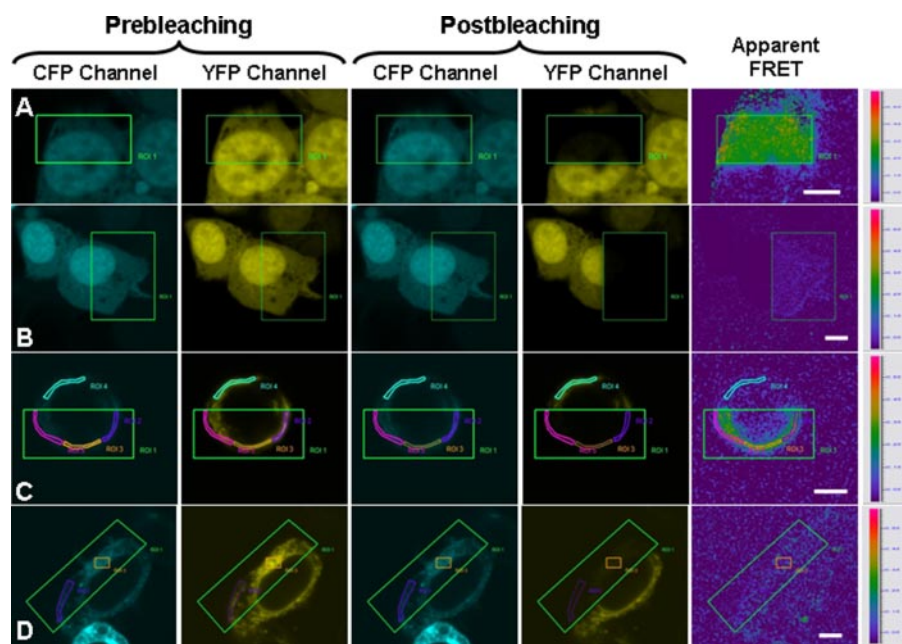


FIGURE 3. FRET acceptor photobleaching of the cells transfected with ECFP-EYFP fusion construct (A), ECFP and EYFP constructs co-transfected separately (B), ECFP-CFTR and α -EYFP-ENaC (C), and ECFP-CLCN1 and α -EYFP- γ -ENaC (D). The area of photobleaching is highlighted by green boxes. ECFP and EYFP images were taken both before and after acceptor photobleaching. FRET efficiency is displayed as a pseudocolor representation. Scale, 5 μ m.

immunoprecipitated with an Ab against GFP. Although this Ab detected ECFP-CLCN1 in both crude lysates and IP of ECFP-CLCN1-expressing cells, an Ab against β -ENaC failed to detect a band in IP of co-expressing cells (top panel and right hand lanes of the bottom panel). However, this Ab did detect β -ENaC in the crude lysates from cells expressing either $\alpha\beta\gamma$ -ENaC alone or those co-expressing ECFP-CLCN1. These data suggest that β -ENaC does not interact with the chloride channel CLCN1. All together, these data suggest that CFTR and ENaC can interact in HEK293T cells and that this interaction is specific.

FRET Measurements by Acceptor Photobleaching—Because ENaC subunits Co-IP with CFTR (Fig. 2), their possible interaction was probed by FRET imaging. FRET occurs when donor and acceptor fluorescent proteins are sufficiently close (≤ 10 nm) that radiationless (*i.e.* not mediated by photons) transfer of energy from donor to acceptor (39–41) can be observed after excitation of the donor (Fig. 1A). Both the rate and the efficiency of energy transfer are directly related to the distance between the donor and acceptor. If the fluorophores are more than 10 nm apart, no FRET will be detected (Fig. 1B).

In acceptor photobleaching FRET, the acceptor is selectively photobleached (36). As a result, if the acceptor is close to the donor and FRET had been occurring, an increase in the fluorescence of the donor is observed because the photobleached acceptor is unable to accept energy. Apparent FRET efficiency (E) is determined from the ratios of ECFP fluorescence emission before and after EYFP photobleaching.

Control FRET Measurements—As a positive control we used ECFP-EYFP fusion protein separated by a 7-amino acid linker (Fig. 1A). The regions of interest in cells expressing both fluorophores were photobleached using the 514 nm laser to 30% of

original intensity. ECFP and EYFP images were taken both before and after acceptor photobleaching. The cells transfected with this construct showed an obvious increase in CFP fluorescence after photobleaching (Fig. 3A), and E averaged $\sim 30\%$ (supplemental Fig. S2). In contrast, our negative control, cells transfected with two unlinked ECFP and EYFP constructs, did not show any change in CFP fluorescence after regional bleaching (Fig. 3B), with an E of $< \sim 1\%$ (supplemental Fig. S2). Also, with acceptor bleaching, another internal negative control is built into each sample, the unbleached areas of the cell. After each bleaching, we compared the bleached area with unbleached regions of the cell to avoid introduction of noise as a result of imaging *per se* and/or drift of the stage. These two controls confirmed our ability to measure FRET by acceptor

photobleaching and always preceded our FRET measurements.

Detection of FRET between CFTR and ENaC—Cells were co-transfected with vectors encoding ECFP-CFTR and $\alpha\beta\gamma$ -ENaC. One of the three ENaC subunits was tagged with EYFP. Also, because α -ENaC is known to form a functional homomeric channel, FRET between CFTR and α -ENaC alone was measured. Fig. 3C shows a set of images acquired before and after regional photobleaching when ECFP-CFTR was co-transfected with α -EYFP. In Fig. 3C the bleached area is shown as a green box. To calculate E , regions of interest were drawn inside the bleached area and were restricted to the delineated plasma membrane. These regions of interest allow us to exclude FRET occurring in the endoplasmic reticulum or other internal compartments. We found an appreciable increase in CFP fluorescence after selective photobleaching with all combinations of ENaC and CFTR, indicative of FRET occurrence. The E averaged $\sim 7\%$, but values as high as $\sim 17\%$ were observed. Thus these values are significant when compared with the negative controls (Fig. 3B) and are comparable to E reported in other FRET studies (42, 43). No increase in CFP fluorescence was observed in non-bleached areas. Supplemental Fig. S2 also demonstrates E values for cells co-transfected with constructs encoding ECFP-CFTR and other ENaC combinations. Again, E was significant relative to the negative control. These measurements indicate that FRET occurs between CFTR and ENaC.

Absence of FRET between CLCN1 and ENaC—Next, we addressed the issue of specificity, *i.e.* whether the observed FRET was specific between CFTR and ENaC or results of random association between two membrane proteins. To address this issue we replaced CFTR with another Cl^- channel, CLCN1 tagged with ECFP (31). To our knowledge, there is no report of association between CLCN1 and ENaC using either electrophysiology or biochemistry. Fig. 3D demonstrates representa-

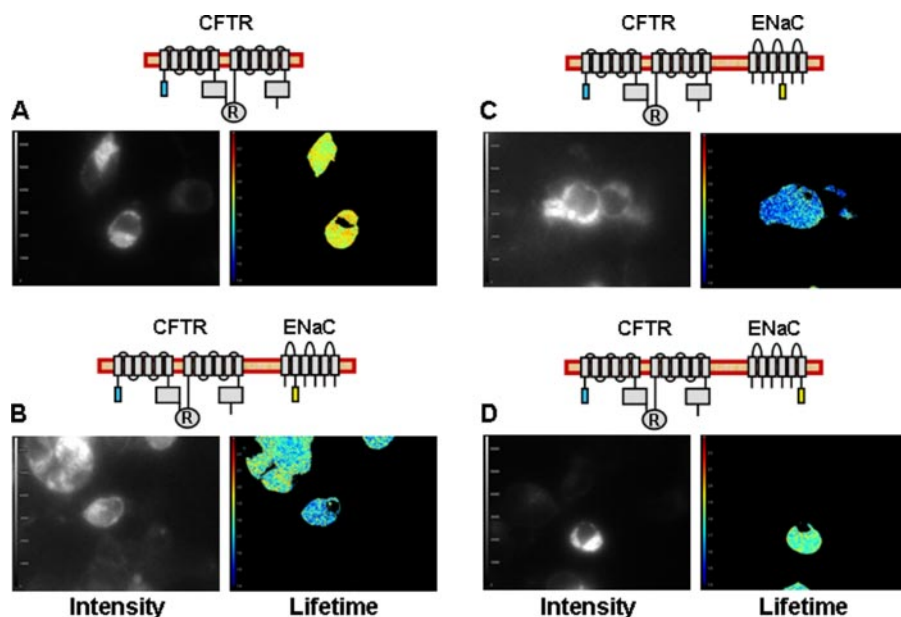


FIGURE 4. FRET measurement by fluorescence lifetime imaging microscopy. The images were taken with cells transfected with ECFP-CFTR (A), ECFP-CFTR and α -EYFP- β - γ -ENaC (B), ECFP-CFTR and α - β -EYFP- γ -ENaC (C), and ECFP-CFTR and α - β -EYFP-ENaC (D) using the LIFA system attached to a Nikon TE2000 microscope. In the resulting images, the intensity is shown in *grayscale* (arbitrary digital unit), and the lifetime is in pseudocolors (nanoseconds).

tive images taken from cells expressing ECFP-CLCN1 and α - β -EYFP- γ -ENaC. No FRET was observed between CLCN1 and ENaC. A summary *bar graph* of E values for other combinations of tagged ENaC subunits and CLCN1 is given in (supplemental Fig. S3). These results, namely the presence of FRET between CFTR and ENaC and its absence between CLCN1 and ENaC, underscore the specificity of the energy transfer between CFTR and ENaC and support the hypothesis of specific CFTR-ENaC interaction.

FRET Measurements by FLIM—As an alternative and independent measure of CFTR-ENaC FRET we used FLIM-FRET. FLIM is fluorescence lifetime imaging microscopy and detects the average time that a group of fluorophores spend in the excited state (44). FRET is marked by a decrease in fluorescence lifetime of the donor fluorophore as its energy is transferred to the acceptor fluorophore. FRET efficiencies (E) are directly calculated from the lifetime donor ratios with and without acceptor. Fig. 4A demonstrates the intensity and corresponding lifetime from phase images of the cells expressing CFTR tagged with ECFP. The FLIM image shows that, in the absence of the EYFP-ENaC, the ECFP tagged to CFTR had an average lifetime (τ_{ECFP}) of ~ 1.9 ns, within a range of previously reported values (45). When ECFP-CFTR and any ENaC subunit (Fig. 4, B–D) tagged with EYFP were co-expressed, a decrease in fluorescence lifetime to τ_{FRET} of ~ 1.7 ns was observed, which reflects the predicted energy transfer from ECFP to EYFP. The values are averaged over 6–10 cells, obtained from 2 or 3 samples. The FLIM-FRET efficiency is calculated as $1 - (\tau_{\text{FRET}}/\tau_{\text{ECFP-N-CFTR}})$ (supplemental Fig. S4).

DISCUSSION

Even though the role of amiloride-sensitive Na^+ pathways in airway CF were delineated at the beginning of 1980s (12, 46),

coupling between CFTR and ENaC only became evident after molecular cloning of ENaC (47–49) following the identification of CFTR (1–3). Soon after the molecular cloning of $\alpha\beta\gamma$ -ENaC subunits, the remarkable ability of CFTR to influence other transporters became evident. This regulatory ability of CFTR is best exemplified by influence of CFTR on ENaC activity (7). Although the evidence overwhelmingly points toward a possible interaction, the nature of this interaction, as well as its existence, is still debated, partly due to contradictory electrophysiological findings and limited biochemical data.

In this study, multiple independent approaches were used to examine the potential interaction of CFTR with ENaC. Using CFTR and ENaC molecules tagged with fluorescent variants of GFP, we were

able to observe a clear delineation of the plasma membrane and strong overlap of the two tagged proteins when they were co-expressed in HEK293T cells (supplemental Fig. S1). We next used Co-IP experiments to determine if the two proteins could interact physically (Fig. 2). Lastly, we used two independent applications of the FRET technique (Figs. 3 and 4) to determine if these two important transport molecules were in close proximity in transfected cells. Using these independent techniques, our findings are consistent with the hypothesis that CFTR and ENaC are in close proximity and likely interact directly.

There are many artifacts of technique that have clouded the literature regarding potential interactions between CFTR and ENaC (24–26). One caveat in the present study concerns the use of an overexpression system. This is an unavoidable complication of the fluorescently tagged FRET-based approach to studying protein-protein interaction. In such systems, there is a possibility of observing nonspecific interactions due to a simple mass balance effect. If occurring, this would be seen as a positive FRET signal due to increased close packing of tagged molecules, where due to high levels expression, there is a FRET interaction in constrained volumes such as in the endoplasmic reticulum or at the plasma membrane. The use of a fluorescently tagged membrane protein such as the sarcolemmal Cl^- channel, CLCN1, can assess the specificity of a positive FRET signal. In our studies there was no evidence to support an interaction between CLCN1 and ENaC subunits (Fig. 3D). The absence of FRET between CLCN1 and our tagged proteins further suggests that the interaction we observed between CFTR and the ENaC subunits is specific.

An overexpression artifact can also be a confounding factor in Co-IP experiments: random interactions may occur due solely to high concentrations of two proteins. This is unavoidable in heterologous expression systems, which are required because endogenous CFTR or ENaC proteins are difficult to

detect. To address overexpression concerns in this system, lysates from cells expressing either CFTR or β -ENaC were mixed *in vitro*. Under these conditions, the two proteins could not be co-immunoprecipitated, suggesting that the Co-IP of CFTR and ENaC was not a random artifact of the overexpression system. It may also suggest that an interaction requires the two proteins to be simultaneously processed and trafficked to the membrane. Although there are known limitations regarding the sensitivity and specificity of the anti-human CFTR (clone 24-1) Ab, the inclusion of appropriate positive and negative controls and confirmation of our findings by Western blot analysis support our conclusions.

It can also be appreciated that the calculated FRET efficiency between CFTR and ENaC proteins is significantly lower than the positive control in which the FRET pair is physically linked together. Although the values are lower, they are significantly higher than those of negative controls. These efficiencies are also comparable to that found by other investigators (42, 43) and may speak to the nature of the interaction. As our experiments focused upon interactions between the N terminus of CFTR and the C-terminal tails of the ENaC subunits, their separation may be greater than that of the 37-amino acid linker found in the positive control but less than that of the 10 nm threshold for FRET. As ENaC trafficking and function is disrupted by manipulations of the N terminus, it is difficult to use FRET to probe the interaction of the N termini of ENaC proteins with CFTR; however, the interaction may be mediated by the N termini of ENaC protein rather than the C termini. It is also very possible that the proteins do not interact directly, but rather through an intermediary, forcing the distance between them to be larger and decreasing the efficiency of FRET. This is rather unlikely, but possible.

Interestingly, the identity of the tagged ENaC subunit had a minimal effect upon the measured FRET efficiency. Because ENaC proteins must form homo- or heteromers to form functional channels, this suggests that the CFTR interacts with a sole ENaC, rather than multiple channels. For example, α -ENaC is known to form a functional homomeric channel; however, there is not an increase in the FRET efficiency between α -ENaC and CFTR as would be expected if multiple α -ENaC subunits interacted with a single CFTR molecule. Although these FRET data cannot easily address the stoichiometry of the interaction, these data suggest a 1-CFTR:1-ENaC arrangement rather than 1-CFTR:Many-ENaC.

The transport of multiple ions and solutes has been proposed to be under the overall control of CFTR, but the potential reciprocal relationship between CFTR and ENaC has been the most widely investigated. However, the present study is the first to present evidence supporting a direct physical interaction between these two important proteins. These studies, which were carried out under conditions of heterologous expression, create the foundation for experiments in cells endogenously expressing both ENaC and CFTR proteins as well as experiments assaying for FRET between CFTR mutants and ENaC proteins. Furthermore, this system allows for mapping of the CFTR and ENaC subunits to define interaction domains or residues. The functional significance of these findings and their implications for CF treatment require further study. However, a

direct functional interaction may suggest the most efficacious therapies would target ENaC as well or place functioning CFTR at the membrane, rather than solely affecting Cl^- transport.

Acknowledgments—We thank Melissa McCarthy, Marina Mazur (University of Alabama at Birmingham), and Jessica Rennolds (Ohio State University) for excellent technical assistance. We also thank Dr. Robert H. Meltzer and Susan J. Anderson for generation of constructs. We appreciate constructive criticisms of Drs. M. Knepper, G. Gy Kovacs, R. H. Meltzer, C. Mazzochi, and W. Vila-Carriles. HEK293T cells were a kind gift of Dr. K. L. Kirk (University of Alabama at Birmingham). Wild-type $\alpha\beta\gamma$ human ENaC cDNAs were a kind gift of Dr. M. J. Welsh (University of Iowa). EGFP-CFTR construct was a kind gift of Dr. B. Stanton (Dartmouth Medical School). ECFP-CLCN1 construct was a kind gift of Dr. Christoph Fahlke (Dept. of Neurophysiology, Medizinische Hochschule Hannover, Hannover, Germany).

REFERENCES

1. Kerem, B., Rommens, J. M., Buchanan, J. A., Markiewicz, D., Cox, T. K., Chakravarti, A., Buchwald, M., and Tsui, L. C. (1989) *Science* **245**, 1073–1080
2. Riordan, J. R., Rommens, J. M., Kerem, B., Alon, N., Rozmahel, R., Grzelczak, Z., Zielenski, J., Lok, S., Plavsic, N., Chou, J. L., Drumm, M. L., Iannuzzi, M. C., Collins, F. S., and Tsui, L. C. (1989) *Science* **245**, 1066–1073
3. Rommens, J. M., Iannuzzi, M. C., Kerem, B., Drumm, M. L., Melmer, G., Dean, M., Rozmahel, R., Cole, J. L., Kennedy, D., Hidaka, N., Zsiga, M., Buchwald, M., Riordan, J. R., Tsui, L. C., and Collins, F. S. (1989) *Science* **245**, 1059–1065
4. Welsh, M. J., and Smith, A. E. (1993) *Cell* **73**, 1251–1254
5. Boucher, R. C. (2004) *Eur. Respir. J.* **23**, 146–158
6. Rowe, S. M., Miller, S., and Sorscher, E. J. (2005) *N. Engl. J. Med.* **352**, 1992–2001
7. Kunzelmann, K. (2003) in *The Cystic Fibrosis Transmembrane Conductance Regulator* (Kirk, K. L., and Dawson, D. C., eds) pp. 55–93, Kluwer Academic/Plenum Publishers, New York
8. Aleksandrov, A. A., Aleksandrov, L. A., and Riordan, J. R. (2007) *Pflugers Arch.* **453**, 693–702
9. Gadsby, D. C., Vergani, P., and Csanady, L. (2006) *Nature* **440**, 477–483
10. Guggino, W. B., and Stanton, B. A. (2006) *Nat. Rev. Mol. Cell Biol.* **7**, 426–436
11. Berdiev, B., and Ismailov, I. (1999) in *Amiloride-Sensitive Sodium Channels: Physiology and Functional Diversity* (Benos, D., ed) Vol. 47, pp. 351–380, Academic Press, San Diego, CA
12. Knowles, M., Gatzky, J., and Boucher, R. (1981) *N. Engl. J. Med.* **305**, 1489–1495
13. Mall, M., Grubb, B. R., Harkema, J. R., O'Neal, W. K., and Boucher, R. C. (2004) *Nat. Med.* **10**, 487–493
14. Stutts, M. J., Canessa, C. M., Olsen, J. C., Hamrick, M., Cohn, J. A., Rossier, B. C., and Boucher, R. C. (1995) *Science* **269**, 847–850
15. Ling, B. N., Zuckerman, J. B., Lin, C., Harte, B. J., McNulty, K. A., Smith, P. R., Gomez, L. M., Worrell, R. T., Eaton, D. C., and Kleyman, T. R. (1997) *J. Biol. Chem.* **272**, 594–600
16. Letz, B., and Korbmacher, C. (1997) *Am. J. Physiol.* **272**, C657–C66
17. Kunzelmann, K., and Schreiber, R. (1999) *J. Membr. Biol.* **168**, 1–8
18. Berdiev, B. K., Shlyonsky, V. G., Karlson, K. H., Stanton, B. A., and Ismailov, I. I. (2000) *Biophys. J.* **78**, 1881–1894
19. Briel, M., Greger, R., and Kunzelmann, K. (1998) *J. Physiol.* **508**, 825–836
20. Ismailov, I. I., Awayda, M. S., Jovov, B., Berdiev, B. K., Fuller, C. M., Dedman, J. R., Kaetzel, M., and Benos, D. J. (1996) *J. Biol. Chem.* **271**, 4725–4732
21. Ismailov, I. I., Berdiev, B. K., Shlyonsky, V. G., Fuller, C. M., Prat, A. G., Jovov, B., Cantiello, H. F., Ausiello, D. A., and Benos, D. J. (1997) *Am. J. Physiol.* **272**, C1077–C1086
22. Ji, H. L., Chalfant, M. L., Jovov, B., Lockhart, J. P., Parker, S. B., Fuller, C. M.,

- Stanton, B. A., and Benos, D. J. (2000) *J. Biol. Chem.* **275**, 27947–27956
23. Konstas, A. A., Koch, J. P., and Korbmayer, C. (2003) *Pflugers Arch.* **445**, 513–521
24. Nagel, G. (2004) *J. Cyst. Fibros.* **3**, Suppl. 2, 109–111
25. Nagel, G., Barbry, P., Chabot, H., Brochiero, E., Hartung, K., and Grygorczyk, R. (2005) *J. Physiol.* **564**, 671–682
26. Nagel, G., Szellas, T., Riordan, J. R., Friedrich, T., and Hartung, K. (2001) *EMBO Rep.* **2**, 249–254
27. Meltzer, R. H., Kapoor, N., Qadri, Y. J., Anderson, S. J., Fuller, C. M., and Benos, D. J. (2007) *J. Biol. Chem.* **282**, 25548–25559
28. Moyer, B. D., Denton, J., Karlson, K. H., Reynolds, D., Wang, S., Mickle, J. E., Milewski, M., Cutting, G. R., Guggino, W. B., Li, M., and Stanton, B. A. (1999) *J. Clin. Invest.* **104**, 1353–1361
29. Grunder, S., Firsov, D., Chang, S. S., Jaeger, N. F., Gautschi, I., Schild, L., Lifton, R. P., and Rossier, B. C. (1997) *EMBO J.* **16**, 899–907
30. Moyer, B. D., Loffing, J., Schwiebert, E. M., Loffing-Cueni, D., Halpin, P. A., Karlson, K. H., Ismailov, I. I., Guggino, W. B., Langford, G. M., and Stanton, B. A. (1998) *J. Biol. Chem.* **273**, 21759–21768
31. Hebeisen, S., Biela, A., Giese, B., Muller-Newen, G., Hidalgo, P., and Fahlke, C. (2004) *J. Biol. Chem.* **279**, 13140–13147
32. Knepper, M. A., and Masilamani, S. (2001) *Acta Physiol. Scand.* **173**, 11–21
33. Masilamani, S., Kim, G. H., Mitchell, C., Wade, J. B., and Knepper, M. A. (1999) *J. Clin. Invest.* **104**, R19–R23
34. Bebok, Z., Varga, K., Hicks, J. K., Venglarik, C. J., Kovacs, T., Chen, L., Hardiman, K. M., Collawn, J. F., Sorscher, E. J., and Matalon, S. (2002) *J. Biol. Chem.* **277**, 43041–43049
35. Cormet-Boyaka, E., Di, A., Chang, S. Y., Naren, A. P., Tousson, A., Nelson, D. J., and Kirk, K. L. (2002) *Proc. Natl. Acad. Sci. U. S. A.* **99**, 12477–12482
36. Karpova, T. S., Baumann, C. T., He, L., Wu, X., Grammer, A., Lipsky, P., Hager, G. L., and McNally, J. G. (2003) *J. Microsc.* **209**, 56–70
37. Helms, M. N., Liu, L., Liang, Y. Y., Al-Khalili, O., Vandewalle, A., Saxena, S., Eaton, D. C., and Ma, H. P. (2005) *J. Biol. Chem.* **280**, 40885–40891
38. Staruschenko, A., Medina, J. L., Patel, P., Shapiro, M. S., Booth, R. E., and Stockand, J. D. (2004) *J. Biol. Chem.* **279**, 27729–27734
39. Clegg, R. M. (1992) *Methods Enzymol.* **211**, 353–388
40. Kenworthy, A. K. (2001) *Methods* **24**, 289–296
41. Selvin, P. R. (1995) *Methods Enzymol.* **246**, 300–334
42. Greeson, J. N., Organ, L. E., Pereira, F. A., and Raphael, R. M. (2006) *Brain Res.* **1091**, 140–150
43. Lai, M., Wang, F., Rohan, J. G., Maeno-Hikichi, Y., Chen, Y., Zhou, Y., Gao, G., Sather, W. A., and Zhang, J. F. (2005) *Nat. Neurosci.* **8**, 435–442
44. Clegg, R. M., Holub, O., and Gohlke, C. (2003) *Methods Enzymol.* **360**, 509–542
45. Kremers, G. J., Goedhart, J., van Munster, E. B., and Gadella, T. W., Jr. (2006) *Biochemistry* **45**, 6570–6580
46. Knowles, M. R., Carson, J. L., Collier, A. M., Gatzky, J. T., and Boucher, R. C. (1981) *Am. Rev. Respir. Dis.* **124**, 484–490
47. Canessa, C. M., Horisberger, J. D., and Rossier, B. C. (1993) *Nature* **361**, 467–470
48. Canessa, C. M., Schild, L., Buell, G., Thorens, B., Gautschi, I., Horisberger, J. D., and Rossier, B. C. (1994) *Nature* **367**, 463–467
49. Lingueglia, E., Voilley, N., Waldmann, R., Lazdunski, M., and Barbry, P. (1993) *FEBS Lett.* **318**, 95–99